UNIVERSITAT AUTÒNOMA DE BARCELONA

FACULTY OF PHYSICS

RADIATION PHYSICS DEPARTMENT

BACHELOR THESIS:

Atmosphere characterization through Barcelona Raman-LIDAR data analysis

Author:
Raúl Ramos Tomás

Director:
Dr. Markus GAUG

Universitat Autònoma de Barcelona - June 2019

I was like a boy playing on the sea-shore,
and diverting myself now
and then finding a smoother pebble or a prettier shell than ordinary,
whilst the great ocean of truth lay all undiscovered before me.

Sir Isaac Newton

One of the basic rules of the universe is that nothing is perfect.
Perfection simply doesn't exist.
Without imperfection, neither you nor I would exist.

Dr. Stephen Hawking

Only those who attempt the absurd can achieve the impossible.

Dr. Albert Einstein

Acknowledgements

This bachelor thesis is dedicated to whole people who help me to reach my dreams, make me who I am today and never give up with me. In special my parents and brother, who supported me in every moment of my life, especially in hard moments like when I was diagnosed with epilepsy one and a half year ago, a very hard moment for me. They trusted in me about doing a physics degree and being involved in science world; and they trusted in my again, when because of the disease I was going to left the degree, and their motivation was indispensable to continue.

I want to thank all the professors, who through the degree, taught me to understand how universe works and make me love physics more than I did. There are to many professors who advised and guided me, but Dr. Lluís Font, and especially Dr. Markus Gaug, who welcomed me in this last year for help me in this thesis, are the ones who did it the most. With Markus I have had a more closed relationship, he treated me as one of his teammates since the beginning and has been very comprehensive with all my doubts and problems. I will never be able to thank you all things you made for me.

In special addition, I want to thank all Barcelona Raman-LIDAR team for the closed treat and the opportunity of be part of an amazing project that will be very important in cosmic radiation studies.

Summary

The main goal of this work is to characterized the atmosphere through the analysis of data collected by the Barcelona Raman-LIDAR located in the Universitat Autònoma de Barcelona campus. Developing a code able to analyze the data, a fit of the received signal and obtaining of extinction and backscattering coefficients were made with the objective of obtaining the LIDAR ratio. The LIDAR ratio makes us capable of understand the atmosphere and know which aerosols can be found.

Characterize the atmosphere is important for the CTA project; a well defined atmosphere makes easy to study Cherenkov radiation generated when the γ-rays go through affected by backscattering and extinction phenomena caused by molecules and aerosols. Moreover, is interesting to know the contribution that aerosols make in the global warming to be alerted on how it evolves.

This projected is carried out by different groups with whom I collaborated. Mainly throughout the year, I was working with Dr. Markus Gaug on code development in order to obtain data that could be analyzed and studied in a physical context. Besides that, after develop the code, the data of a specific day was chosen to study the atmosphere. After processing the data of 19th July 2018, I analyzed it and using the LIDAR ratio data from [2] the atmosphere was characterized.

Contents

1 Introduction

1.1 What is CTA?

The Cherenkov Telescope Array, usually called CTA by its initials, is a worldwide scientific project whose main purpose is to build a new generation of gamma-ray detectors. These new generation detectors have an energy range from some tens of GeV to more than 300 TeV. CTA will consist of more than 100 telescopes installed at two sites, one in the northern and another in the southern hemisphere to ensure full-sky coverage.
The northern hemisphere array focuses on the low-mid-energy range from 20 GeV to 20 TeV for detection of mainly extragalactic sources, while the southern hemisphere array focuses on the entire energy range covering gamma-ray energies from 20 GeV to 300 TeV to detect mainly galactic sources.

In this project more of 200 institutes in 31 countries, among them Spain, are collaborating. In our country a lot of institutes are members of the CTA community, like the Institut de Física d'Altes Energies (IFAE) and the Universitat Autònoma de Barcelona.
These institutions collaborate in establishing the science goals of CTA, they are involved in the array design and supplying components. In fact, IFAE and UAB, and recently also a Slovenian group, are finishing to build a Raman LIDAR for CTA, whose final destination is La Palma.

The main purpose of building a Raman LIDAR for CTA is to measure the energy of electromagnetic cascades more precisely than previous installations, like MAGIC. Hence, they need a more accurate atmospheric characterization for this aim. The Barcelona Raman LIDAR is an integral part of CTA.

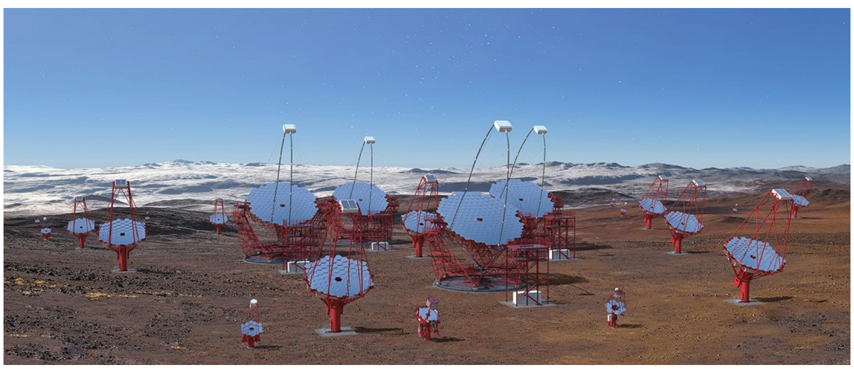

Figure 1: Image taken from CTA website that shows how looks a Cherenkov telescope Array.

1.2 The Cherenkov effect and Cherenkov telescopes (IACTs)

It is known that much of the radiation that reaches our planet is thermal origin and its range extends to about a few keV. Nevertheless, universe produces also non-thermal radiation that reaches the Earth and which extends up to > 100 TeV.
This kind of radiation arrives to Earth because of different phenomena like cosmic rays, which are basically charged particles. When these particles strike over the atmosphere atoms and molecules, new particles are produced in consequence. These secondary particles produce new particles successively originating a cascade of charged particles.

If we suppose a charged particle, like an electron, traveling through a dielectric medium at a speed comparable to the phase velocity of light in that medium, the medium will be polarized as the particle travels through it. If the speed is slow this effect is not produced because the medium reacts at the same speed as the particles travels. On the other hand, if the speed of the charge particle is fast, a net dipole will be created which moves at the speed of the particle [1].

In the process of creation and destruction of these dipoles radiation is emitted. Generally, the dipole electromagnetic waves interfere destructively between them. Only if the charged particle travels faster than phase velocity of light inside the same medium, the interference is constructive and each dipole increases the amount of radiation emitted. This phenomenon is called Cherenkov radiation.

This kind of radiation is emitted under a certain angle described as:

$$\cos\theta = \frac{l_w}{l_p} = \frac{c/n \cdot t}{\beta ct} = \frac{1}{\beta n} \tag{1}$$

Where l_w and l_p are the paths of the wave and the particle travel in a time interval, t, respectively. The value n is the refraction index which depends on the medium where the particle travels. Finally, we can define β as the speed of the particle relative to the speed of light in vaccum, c.

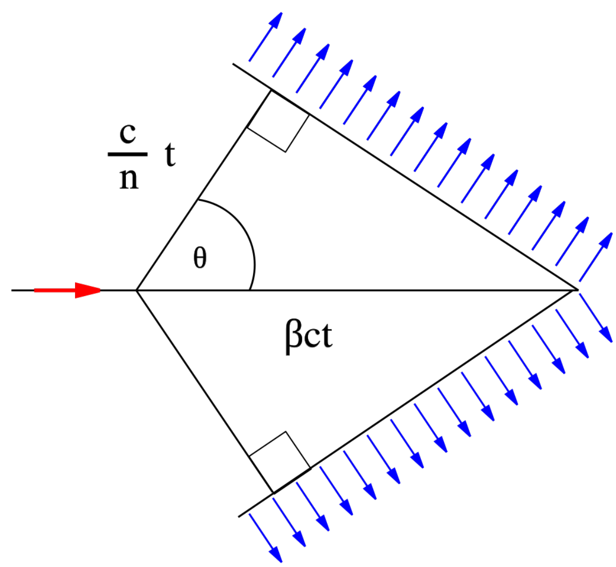

Figure 2: Figure extracted from Wikimedia Commons that shows how Cherenkov radiation is produced along dipole wavefront.

The detection of Cherenkov radiation is fundamental for the study of high energy particles, particularly γ-rays, and know about different physics phenomena. It can be detected through different types of detectors like telescopes.
For a time, there was no way to detect extraterrestrial γ-rays because technology was not good enough. Since the 50s, when the first satellite was launched and collected data about γ-rays among others, the detectors and the way of collect information have evolved. Only in the 1990s, ground-based γ-rays detectors became feasible through the invention of IACTs.

A factor to keep in mind when we want to detect γ-rays from galactic or extragalactic sources is that the γ ray flux decreases fast. If we take this in satellites and other space detectors, we can see clearly how inefficient are they because of the area they need to cover to detect this radiation. Instead, a ground-base detector, usually called IACT, is more efficient because of the atmosphere collects this radiation acting as a detection medium and enabling IACT to detect γ-ray particles at energies inaccessible for space detectors. They detect and image the Cherenkov radiation generated by the charged particle cascade, called extensive air shower, which it starts at an altitude of 10-20 km.

IACT instruments are made up of a large segmented mirror which reflects the Cherenkov radiation towards an array of photomultipier tubes. This kind of fast electronic devices are responsible to convert the incident photons into an electrical signal, amplifying and recording the shower track image.
An array system of this kind of detectors improves further sensitivity, angular and energy resolution.

1.3 Atmospheric characterization and its importance for IACTs

Atmospheric conditions become important at the moment that Cherenkov radiation is affected by backscattering and attenuation phenomena and it happens in the moment that the γ-rays enters the atmosphere and the air-shower starts.
So, it is important to measure the attenuation of Cherenkov radiation within the atmosphere, because Cherenkov light is attenuated when travels through the atmosphere. Resolve measurements of physical and optical properties of particles such as surface concentration, volume, mass concentration, particle size and volume of extinction coefficients are so important, they only can be carried out with a LIDAR [2].

The atmosphere is constituted by different gases, mainly oxygen and nitrogen, and they influence the opening angle and attenuation of Cherenkov radiation. Nevertheless, there are another important component in the atmosphere with an important role, the aerosols. Although they are a minor component of the atmosphere, they have a huge influence on air quality, clouds and Earth's radiation among others. There exists many different types of aerosols like continental aerosols from pollution, water aerosols, dessert dust or icy dust. The type of aerosols that can be found depends on our geographical situation; for example, in our country, dessert dust from Sahara can affect us, but icy powder from any earth pole can't affect us [3].

When the light travels along a polarizable medium like the atmosphere, excites its molecules absorbing a quantum of light and making them behave like an oscillator. Immediately after its excitation, the absorbed photon, with the same frequency and wavelength that when the photon fell upon the molecule, is emitted. It is an elastic scattering of radiation and is known as Rayleigh scattering.
Rayleigh scattering has an important effect when the size of the molecules are much smaller than the wavelength of the scattered radiation. [4]

We can find an expression for the Rayleigh scattering cross-section for unpolarized light within the atmosphere. Starting off with the equation which define scattering cross-section for a particle of a molecular gas:

$$\frac{d\sigma_R(\theta)}{d\Omega} = \frac{\pi^2(n^2-1)^2}{N^2\lambda^4}\frac{\cos^2(\theta)+1}{2} \tag{2}$$

where θ is the angle between by our considered direction and the propagation direction of the light, λ is the wavelength of the light, n is the refraction coefficient of the medium and N is the density of refractors. Considering a particle density inside the atmosphere we can obtain the absorption and its definition. We can define the volume backscattering coefficient as $\beta = \sigma \cdot n(h)$, where the last term is the particle density of the atmosphere regarding to height.
Defined in [5], the Rayleigh scattering cross-section volume for unpolarized light is:

$$\beta_{mol}(180^o,\lambda,h) = \frac{6\pi^2(n_s^2-1)^2}{N_s\lambda^4(n_s^2+2)^2}\cdot\left(\frac{6+3\rho(h)}{6-7\rho(h)}\right)\cdot\frac{P(h)}{P_s}\cdot\frac{T_s}{T(h)}\cdot\frac{3}{4}\cdot\left(\frac{2+2\rho(h)}{2+\rho(h)}\right)\cdot\left(1+\frac{1-\rho(h)}{1+\rho(h)}\right) \tag{3}$$

Analyzing this formula we can see a resemblance between Eq. 2 and the four first terms of Eq. 3, but for the last one has been considered the *King correction*. This correction accounts for the anisotropy of air molecules. Also, another correction can be seen, it corrects the different air density for each height measured through pressure and temperature. Whereas the last two terms agree with *Chandrasekhar corrected phase function* from [6]. Also, the constant values make reference to the refraction index, n, the density of molecules per volume unit, N_s, the wavelength; λ and the depolarization coefficient, ρ. In addition, the magnitudes of equation (3) are $\mathrm{m}^{-1}\mathrm{Sr}^{-1}$.
Moreover, we can use the relation $9\cdot(n^2-1)^2/(n+2)^2 \approx 4\cdot(n-1)^2$ to simplify calculus. It should be said that King's factor will be different for each mentioned wavelength.

1.3.1 Standard atmosphere consideration

Assuming a clean-dry air, where light-atmosphere interaction is caused by Rayleigh scattering, the latter shows a dependency on chemical composition and density of air molecules.
Looking back of the Rayleigh scattering section-cross volume, Eq. 3, for a standard temperature and

pressure, T_s=288,15 K and P_s=101325 kPa respectively, the constant value of density of molecules is N_s=2,5469·10^{25} m^{-3}. [7]

Taking into account that the values of n and ρ depends on light wavelength, pressure, temperature and other factors like humidity and CO_2 concentration, [8], these values will be different for the initial laser beam wavelengths, elastic and Raman, and the backscattering corresponding ones. For example, for 355 nm wavelength, n=1.00028543 and ρ=0.0304, and its backscatter wavelength of 387 nm, n=1.00028321 and ρ=0.0297; the latter wavelength line is about 532 nm, with n = 1.00027791 and ρ=0.0282, and its backscatter wavelength 607 nm, with n=1.00027658 and ρ=0.0279.

2 The Raman-LIDAR project

2.1 What is a LIDAR?

LIDAR is a technology for measuring positions of physical objects by illuminating the target with pulsed laser light and measuring backscatter pulse with a sensor. Its acronym means *Light Distance And Ranging.*
When we launch a pulse, it scatters in all directions because of interactions with the atmospher's molecules and aerosols. Therefore, reflected backscattered light is detected by a LIDAR system; it comes from the molecules, aerosols, clouds and another atmospheric particles that act like a mirror for the pulse. As discussed above on atmosphere characterization, the backscattered light may have a different wavelength than incident light.
After receiving the backscatter light, the LIDAR system picks up the light and focuses it on a photodetector that measures the scattered light as a function of time.

To be able to explain how a LIDAR system works, we need to present the LIDAR equation. Eq. 4 expresses the portion of the emitted power that is backscattered and detected by the system as a function of its range, r, and laser wavelength, λ.

$$P(\lambda, r) = P_0(\lambda) O(r) \frac{A}{r^2} C(\lambda) (\beta_{\mathrm{mol}}(\lambda, r) + \beta_{\mathrm{aer}}(\lambda, r)) \exp\left(-2 \int_0^r (\alpha_{\mathrm{mol}}(\lambda, r') + \alpha_{\mathrm{aer}}(\lambda, r')) dr'\right) \tag{4}$$

where $P_0(\lambda)$ is the emitted power of laser wavelength λ, $O(r)$ is the overlap function, A is the effective area of the telescope, $C(\lambda, r)$ is a system constant accounting for the transmission of photodetector, β_{mol} and β_{aer} are the backscattering coefficients of air molecules and aerosols, respectively, and α is the extinction coefficient. To solve this equation, we need to determine the backscattering and attenuation coefficients, β and α. However, we must consider the case in which the overlap function, $O(\lambda, r)$ is 1. This happens when the LIDAR detector field of view and the laser image completely overlap. In this case, we can rewrite Eq. 4:

$$P(\lambda, r) = P_0(\lambda) \frac{A}{r^2} C(\lambda, r) \beta(r) \exp\left(-2 \int_0^r \alpha(\lambda, r') dr'\right) \tag{5}$$

where β is the sum of the backscattering coefficients and α the sum of extinction coefficients. Using logarithms to remove the exponential term and writing the equation in a differential form, we obtain:

$$\frac{dS}{dr} = \frac{1}{\beta} \frac{d\beta}{dr} - 2\alpha \tag{6}$$

where S is the Napierian logarithm of $P(\lambda, r) r^2$. We can easily notice this equation can not be solved without extra information because β and α are unknown. That is the reason why is necessary define a relation between them, the LIDAR ratio, α/β, which must be known by a LIDAR system. Nevertheless, there are methods to obtain the previous coefficients which will be discussed in the following sections.

2.2 The Raman effect

The Raman effect, usually called Raman scattering, describes the inelastic scattering of light by molecules which are excited to higher energy levels. When scattering is produced by a medium, the bigger fraction of it is elastic scattering. However, a small fraction is scattered inelastically. This inelastic scatter causes that the scattered photons have a different wavelength than the incident ones. This difference between the wavelengths can be traduced in energy terms, it is the energy required to excite a molecule to a higher vibrational mode.

According to the difference of energy due to the excitation energy, it is possible to have lower (Stokes) or higher (Anti-Stokes) frequencies in relation with the incident one. It is a correspondence between temperature and frequency. Since atmospheric temperature is cold enough as to not find the molecules in vibrational states, the light only can be backscattered with less energy than the incident light. However,

vibration is not the only way to have Raman scattering, rotational transition are another phenomenon that produce this scattering.
Raman scattering depends on molecules polarizability like Rayleigh scattering. Therefore, there is a net dipolar moment and it can give some inertia and molecular structure information. [9]

2.3 The Raman-LIDAR technique

A Raman-LIDAR works like an elastic LIDAR, using laser beam pulses to study the atmosphere. Raman scattering is produced when the pulse interacts with atmospheric molecules like nitrogen, oxygen or water vapor. The difference between the incident wavelength and the scattered one is unique for each molecule. Therefore, one can know which molecule has produced the scattering.

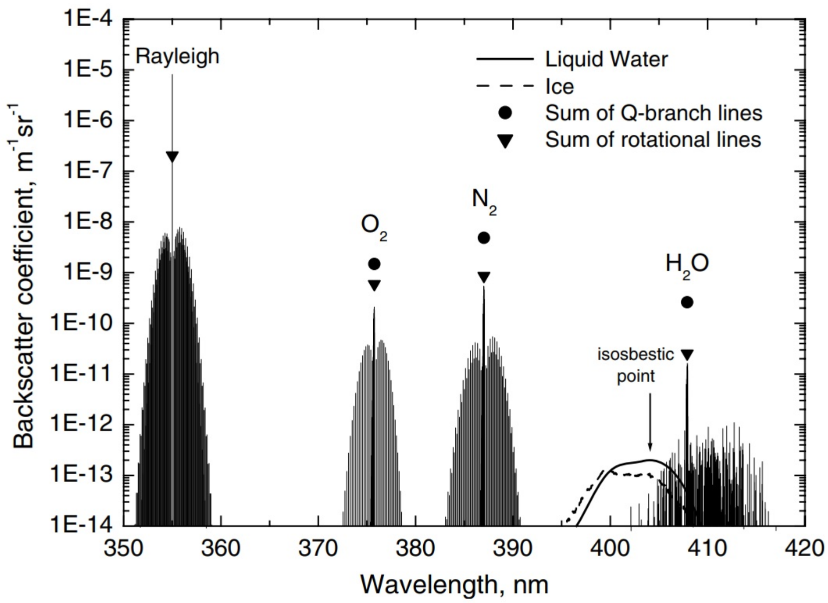

Figure 3: Figure that shows elastic and Raman backscattering coefficients as a wavelength function for basic atmosphere compounds. [10]

Figure 3 shows us in which wavelength we can find the maximum value of the backscattering coefficient of each molecule if the atmosphere is illuminated at 355 nm. This maximum value is the integral over all vibration modes. Looking for Rayleigh scattering we can see the maximum at 355 nm which value is used in our LIDAR system. Besides, the graphic shows that the Raman line for nitrogen is most intense with a higher backscattering than the other lines. That is logical because nitrogen is the most abundant compound of the atmosphere and a Raman LIDAR usually uses the wavelength corresponding to the maximum backscattering coefficient, whose value is about 387 nm. In addition, Raman LIDARs use Raman lines with a short wavelength to increase the signal due to the Raman cross-section is proportional to λ^{-4}.

Taking into account and applying this in Eq. 4 Raman-LIDAR equation is obtained:

$$\begin{aligned} P(\lambda_R, r) = P_0(\lambda_R) O(r) \frac{A}{r^2} C(\lambda_R) N_R(r) \frac{d\sigma_{\lambda_R}(\pi)}{d\Omega} \cdot \\ \cdot \exp\left(- \int_0^r (\alpha_{\mathrm{mol}}(\lambda, r') + \alpha_{\mathrm{aer}}(\lambda, r') + \alpha_{\mathrm{mol}}(\lambda_R, r') + \alpha_{\mathrm{aer}}(\lambda_R, r') dr' \right) \end{aligned} \tag{7}$$

where N_R is the number of nitrogen molecules per volume unit, $d\sigma_{\lambda_R}(\pi)/d\Omega$ is the cross-section, for $\theta = \pi$, with a constant value, and extinction coefficient appears for elastic and Raman lines.

Raman-LIDARs technical necessities are so different from regular LIDARs because of the low intensity of the Raman backscatter signals. Their basic requirements are a high-power laser, a highly efficient receiving and detection system, and multiple detection channels for the Raman line and the elastic line. [10]

A laser for a Raman-LIDAR does not need to emit in specific wavelengths or high spectral purity, it only needs a high average laser power and a wavelength emission range between 320 nm and 550 nm. Looking at Figure 3, in the mentioned emission range of the laser, the maximum laser backscattering peaks are found. Firsts Raman-LIDARs had a relatively low average power compared with current lasers, causing that atmospheric Raman measurements were limited to ranges of about 2 km. Nowadays, pulsed lasers with high average power in the visible and ultraviolet spectral region are used. There are many types of lasers which work in this range, but Nd:YAG laser is the workhorse for current Raman-LIDARs. Their usual wavelength is 355 nm, obtained by frequency-tripling techniques from 1064 nm. The new generation of lasers allow current Raman-LIDARs to analyze the middle and upper troposphere.

The detection system compounds are a telescope, a subsequent receiver optics system and other detectors like photomultipliers. Roughly speaking, Raman-LIDAR telescopes need bigger mirrors to focus the limited Raman lines that they receive. Its size depends on the necessities that our Raman-LIDAR needs to study atmosphere but generally are of the order of 0,5-1 m of diameter. Sometimes, some Raman-LIDARs use bigger mirrors, like CTA Raman-LIDAR, which mirror is about 1,8 m of diameter.
The receiver optics system is optimized for high transmission of Raman signals. The elastically backscattered light in Raman channels must be suppressed. Sometimes a suppression factor is necessary in nitrogen and water-vapor Raman channels and is achieved using dichroic beam splitters. Dichroic beam splitters reflect light of a certain wavelength range with high efficiency whereas they transmit light of other spectral regions.
Photomultipliers are tipically used in Raman-LIDARs detection system requiring a high quantum efficiency and low noise. Their goal is to get the number of counts per range gate and unit time with the best possible efficiency and register the data. In addition, when working under daylight conditions and in near range, Raman signals allow analog detection, and combining analog and photon-counting detection can help to increase the dynamic range of the system.
The reason why nowadays the Raman-LIDAR technique turns out to be very stable and robust for routine and automated observations is because the set of instruments allow a good atmosphere study.

2.4 Necessities of working in multiple scattering lines at Raman-LIDAR

The key to characterize completely the atmospheric aerosols is an exhaustive investigation on chemical and physical properties of particles. Likewise, information about their spatial and temporal behavior, like extension or global distribution are important. It is important to know physical aerosol properties in relation with electromagnetic radiation, like Cherenkov radiation, such as their reflection, transmission and emission. [11]
As discussed above, Raman-LIDARs use multiple detection channels in different wavelengths to study the atmosphere. Every wavelength gets reflected by atmosphere through elastic backscattering. Every compound of the atmosphere does so, molecules and aerosols. The latter does so according to size and shape, making it difficult to study their optical behaviour. The different used wavelengths suffer an extinction in the round trip.

Besides of suffering elastic backscattering, molecules and aerosols that form atmosphere suffer Raman backscattering. Each of these molecules suffers Raman backscattering with its own wavelength, i.e., aerosols suffer Raman backscattering at different wavelengths. With the support of a polychromator whose purpose is to guide the laser light, the atmospheric extinction can be studied without an aerosol backscattering model.

The main necessity to work with multiple wavelength channels is because of the great dependence that aerosols extinction have on wavelength. There is a parameter, called Angström parameter, that describes the extinction coefficient variation with wavelength. Angström parameter appears in equation 8 as a negative exponential:

$$\frac{\alpha(\lambda_1)}{\alpha(\lambda_2)} = \left(\frac{\lambda_1}{\lambda_2}\right)^{-\text{Å}} \tag{8}$$

The bigger λ value, the smaller extinction coefficient. This parameter has a little dependence on λ, it does not always have the same value.

2.5 Barcelona Raman-LIDAR

The Radiation Physics Unit of the UAB Physics Department, Insitut de Física d'Altes Energies (IFAE) in collaboration with a Slovenian group of physicists and engineers participate in the CTA project. Their work is based on calibrating and studying the atmosphere through their own Raman-LIDAR project, called the Barcelona Raman-LIDAR. For several years, they have been working on the LIDAR design, construction and data analysis with Dr. Markus Gaug as the head of the group. Several students were active members in the group while writing their bachelor thesis. This LIDAR will be located at the El Roque de los Muchachos at La Palma.

The Barcelona Raman-LIDAR is a LIDAR which works with four wavelength lines to cover the CTA optical sensibility between 300 nm and 650 nm. There are two elastic lines of 355 nm and 532 nm, and two Raman lines of 387 nm and 607 nm. These two lines are Raman lines of nitrogen because it is the majority component of the atmosphere.

The whole electronic and optic system is protected by a container, its function is to protect it from rain and dust. The container opens sideways due to a hydraulic system and is qualified to its transport. Regarding the telescope, it has a spherical mirror of 1,8 m of diameter with little roughness of the order of nanometers. Its reflectivity was measured, it was about 95% when purchased, but has decreased about 50% after 10 years of operation. Nevertheless, it preserve the roughness and other optical properties. As all mirrors, the Barcelona Raman-LIDAR does not create perfect images, they are affected by aberrations. By means of experiments the size of a punctual source was measured and the results revealed that almost all the light was contained in a 6 mm diameter circle. The mirrors are protected with polystyrene petals. The telescope has zenit and azimuthal movement due to a mechanical system that also holds the laser.
The laser is a Nd:YAG (Neodymium Doped Yttrium Aluminium Garnet), the typical laser in current LIDARs, a solid state laser. This kind of laser emits a pulsed beam of 1064 nm and with non-linear crystals we get the UV and green wavelengths. Applying a beam dump photons of 1064 nm wavelength are stopped, reflecting only photons of 355 nm and 532 nm.
After the pulsed beam is launched to the atmosphere, light is collected by the main mirror and focused to be guided to the polychromator. Its function is to separate the four wavelengths and focus them on to four different photomultipliers, which correct the signal in an amplified electrical signal.
Finally, a system called LICEL analyzes this information, providing digitized data that can be further processed.

3 Data analysis and atmosphere characterization

3.1 Data processing

The data output consists of photon counts from the photomultiplier with respect to the distance from the detector. The return signal is then corrected by a r^2 factor because of its dependence on the solid angle and the logarithm of that product is normally shown. Because of the exponential decrease of the density of air molecules, and hence scatters, over distance.

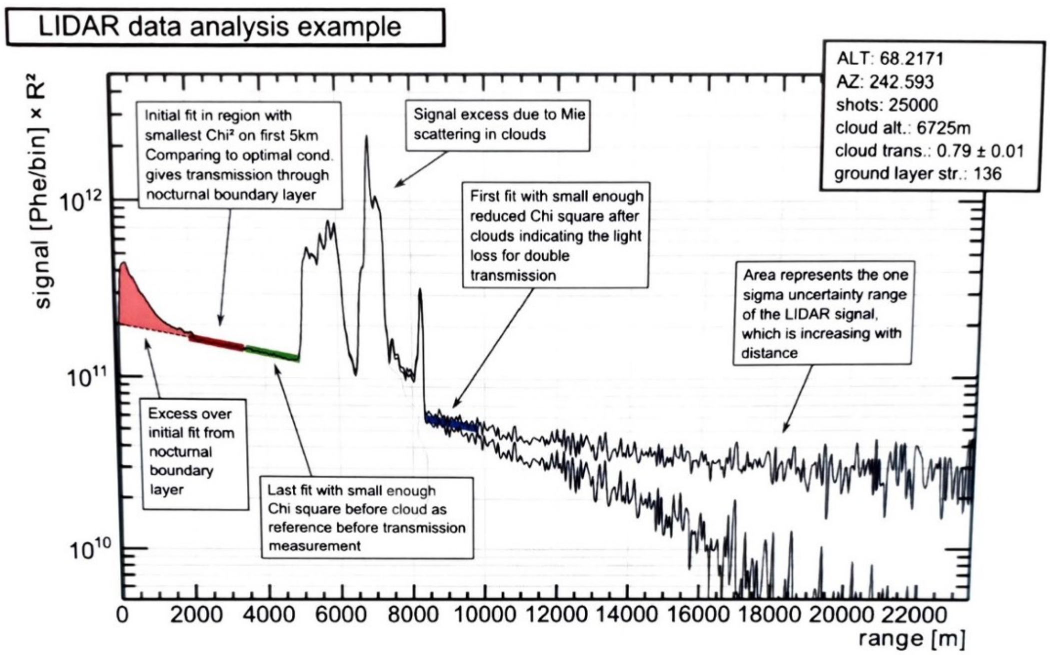

Figure 4: An example of a range-corrected signal from an elastic channel of a LIDAR. [12]

Figure 4 shows an example of a range-corrected output signal. At the beginning, in the first hundred of meters, there is an abrupt increase of counts when the backscattered light enters the field of view of the detector only after the pulse has traveled some distance. This is followed by a decrease over some kilometers because of the relation between backscattered light and the planetary boundary layer. Afterwards, an increase due to the aerosol interaction with pulsed beam and a peak related with Mie scattering in clouds is visible, that cause an increase of backscattered photons. Finally, there is a linear behaviour with noise due to molecular extinction.
This graphic shows some additional information. The amount of light is extinct by clouds, is seen where the counted photons are lower than before the cloud peak.

In the following, before showing and analyzing the results obtained during the night of 19th July 2018, I will introduce some aspects of how the signal of a night without clouds looks like and some aspects about filtering background noise to obtain a smoothed graphic to analyze.
A standard night, like almost all Barcelona's summer nights, shows a signal without scattering due to clouds. After the first excess related to planetary boundary layer, a linear behaviour is observed. Thus, it is expected that high optical transmission values are found because the lack of clouds allows to receive the light without being disturbed. The only cause of aerosol extinction is the boundary layer and possible further layers of dust above it.

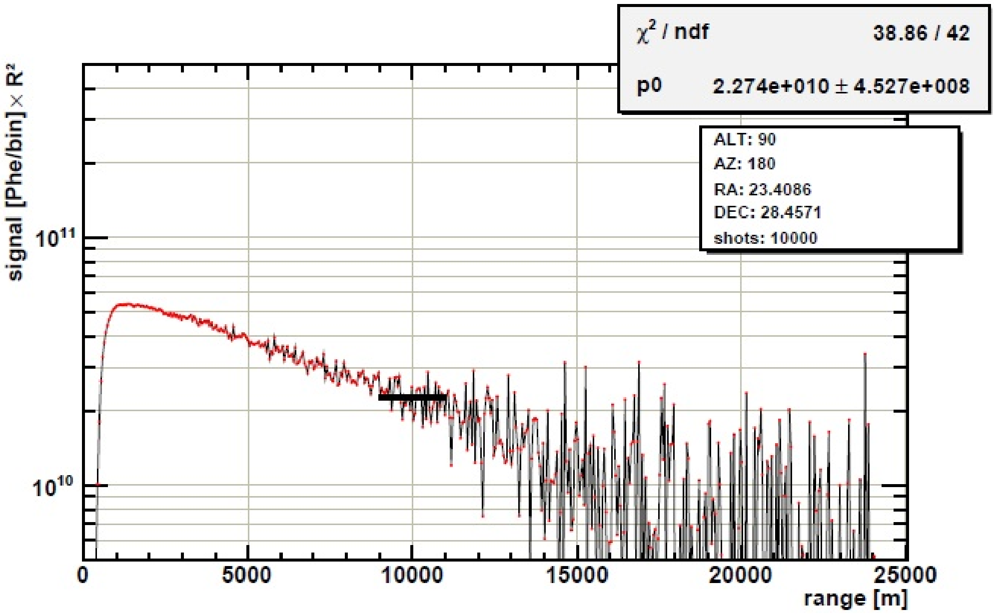

Figure 5: An standard clean night atmospheric signal profile from an elastic backscatter channel. [12]

Figure 5 shows how a standard clean night profile looks without filtering to reduce background noise and smothering. In this figure, it is easy to see that planetary boundary layer is normally below 2,5 km. In this case, a Rayleigh fit is possible above 3 km. This fit is obtained when the molecules interact with the laser and backscatter it, i.e., the backscattering of aerosols is not taken into account. Otherwise, we can have a Raman fit, if we take into account only nitrogen molecules and extinction from molecules and aerosols.
Rewriting Eq. 5 in logarithm terms, we obtain:

$$S(r) = \ln(N(\lambda, r) \cdot r^2) = \ln(N_0 A l) + \ln(\beta(r)) - 2\int_0^r \alpha(r')dr' \tag{9}$$

where l is a correction factor for the pulse length. By using altitude approximations, respect to sea level, Eq. 3, can be rewritten as:

$$\beta_{\mathrm{mol}}(\theta = 180^o, \lambda, h) \approx \beta_0 \cdot \exp(-H/H_{0,n}) \tag{10}$$

Where $H_{0,n}$ is the average scale height of the molecular density of air in the troposphere with a value of about 9,8 km and the relation between extinction and backscattering coefficients is expressed as $\alpha \approx 8\pi\beta/3$.[13]. So, using approximation 10 on Eq. 9, we obtain for the case of no aerosols:

$$S(r) \approx C - s \cdot H + k \cdot H^2 + ... \tag{11}$$

Where C is the overall detection efficiency as y-intercept and s is the slope. Actually, since k is of the order of 10^{-9}, the second order of Eq. 11 will not be used in Rayleigh fitting approximation expressed hereafter.
So finally, combining the logarithmic expression of $S(r)$ with equation 11 on first order, the Rayleigh fitting equation, which allows obtain C and s values, is obtained:

$$\ln(N(r) \cdot r^2) = \ln(C) - s \cdot r \tag{12}$$

Nevertheless, there are other possible ways to obtain a more worked profile than using Eq. 10. In this study, the backscattering coefficient, $\beta(180^o, \lambda, h)$, was obtained using an ECMWF model, the Global

”Data Assimilation System”. This type of models are used global forecasts and climate reanalyses among others, showing how the weather is most likely to evolve.

Once equations and plots of the general behaviour are expressed and after data taken with Barcelona Raman-LIDAR, the plots obtained with a code implementation in Python language will be shown and analyzed in the next lines. Also, not only the corrected signal plot will be analyzed; extinction coefficients for determinate which aerosols affect the Barcelona area and LIDAR ratio will be treated.

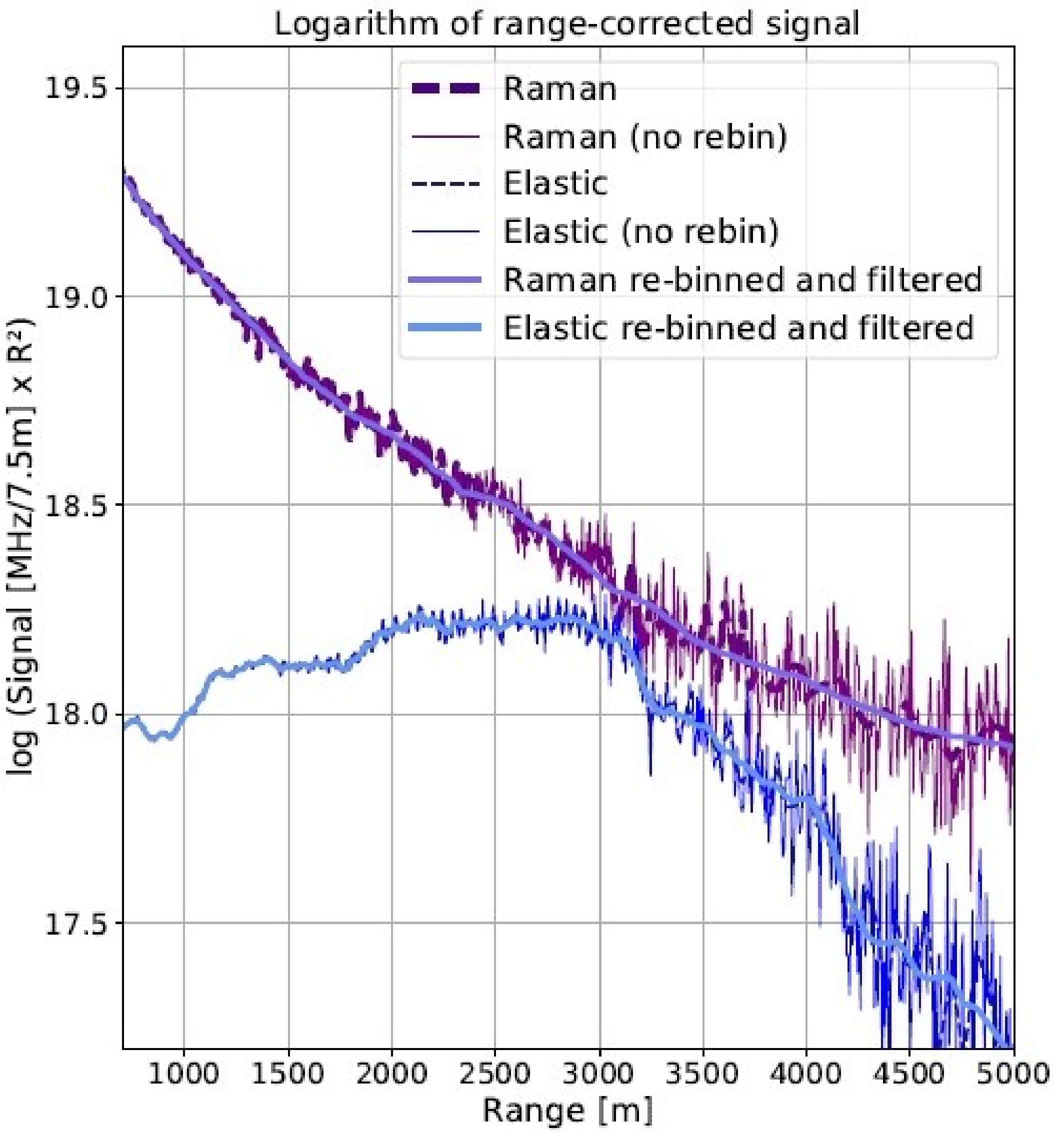

Figure 6: The corrected signal obtained in a clear day on 19th July 2018 with the Barcelona Raman-LIDAR launching 500 shots with the pulsed laser. Purple continuous line shows the Raman backscattered corrected signal with an applied Savitzky-Golay filter; the blue continuous line shows the elastic backscattered.

Figure 6 shows the analysis of the range corrected signal for data taken with the Barcelona Raman-LIDAR. The analysis is implemented with a code with an applied filter, the Savitzky-Golay filter.
A Savitzky-Golay filter is a digital filter that is applied to a set of digital data points with the purpose of smoothing the data to increase the precision without distorting the signal tendency.
The extinction of signal decays exponentially with height due to aerosol and molecules density. At low

altitude there is a higher particle density than at high altitudes. Comparing the Raman filtered line with the elastic filtered line in the firsts 2,5-3 km, it is deduced, from the profile fluctuations, that the Rayleigh scattering is produced due to the existence of an aerosol layer. Raman filtered line is represented with a smooth exponential decay, i.e., the signal decreases with the increase of altitude. Instead, Rayleigh filtered line has a fluctuating behavior. After this region, at 3 km above the ground, Rayleigh filtered line fits perfectly as a smooth decay due to the low density of particles and the lack of aerosols at this altitude, like Raman filtered line. There, both scatterings can be produced. Actually, Rayleigh filtered line would be over Raman filtered line, in a signal with a value of about 22. The reason why the signal was decreased artificially is the saturation of the signal, what hindered the data analysis.
From here we present some typical physical characteristics of particles according to the zone where they are found. Particles below 2,5-3 km are bigger than the wavelength of the backscattered photons. In addition, they have no regular shape, their structure is messy and amorphous. Although there is a main compound, aerosols are not pure; they are mixtures. From 3 km until the signal extinction, particles can have different sizes, shapes and compositions.
Analyzing generally the corrected signal intensity, it is clear that the amount of backscattered light decreases with height because there are less particles to interact with.

As additional information, figure 6 begins at 500 m because below this distance, the received signal was saturated.

3.2 Aerosol extinction and backscatter coefficients

In the Raman-LIDAR technique the Raman backscatter signal is affected by aerosol extinction but not by aerosol backscatter interactions. Therefore, analysis of the Raman-LIDAR signal alone permits the determination of the aerosol extinction coefficient. [3]
From Raman-LIDAR equation, Eq. 7, considering that overlap function is unity among other cross-section considerations, it can be rewritten as:

$$\alpha(\lambda_0, r) + \alpha(\lambda_R, r) = \frac{d}{dr} \ln\left(\frac{N_R(r)}{r^2 P(\lambda_R, r)}\right) \tag{13}$$

where N_R are nitrogen molecules per volume unit and $d\sigma_R(\lambda)/dr=0$ has been used. Splitting the extinction coefficient into an aerosol and a molecular part and assuming a wavelength dependence of the aerosol extinction of $\alpha_{\text{aer}}(\lambda,r) \propto \lambda^{-k}$, Equation 13 can be solved for the aerosol extinction at the emitted laser wavelength as:

$$\alpha_{\text{aer}}(\lambda_0, r) = \left(\frac{d}{dr} \ln\left[\frac{N(r)}{r^2 P(\lambda_R, r)}\right] - \alpha_{\text{mol}}(\lambda_0, r) - \alpha_{\text{mol}}(\lambda_R, r)\right) / \left(1 + \left(\frac{\lambda_0}{\lambda_R}\right)^k\right) \tag{14}$$

where k is the Angström parameter. The values of molecular extinction can be calculated from Rayleigh scattering coefficients and atmospheric density profiles. With the detection of the Raman scattered light, independent aerosol extinction profiles can be determined. This information can be used to derive the aerosol backscatter without any assumption on the extinction-to-backscatter ratio, known as LIDAR-ratio, related directly to microphysical properties of the particles. The backscatter profile is then calculated by forming the ratio of the elastic and Raman backscattered signals at height r and a calibration height r_0.
Nevertheless, there is an equation which defines the aerosol backscattering coefficient at the emitted laser wavelength obtained combining equations 4 and 7:

$$\beta_{\text{aer}}(\lambda_0, r) = -\beta_{\text{mol}}(\lambda_0, r) + [\beta_{\text{aer}}(\lambda_0, r_0) + \beta_{\text{mol}}(\lambda_0, r_0)] \cdot \frac{P(\lambda_R, r_0) \cdot P(\lambda_0, r) \cdot N_R(r)}{P(\lambda_0, r_0) \cdot P(\lambda_R, r) \cdot N_R(r_0)} \cdot \frac{\exp\left[-\int_{r_0}^{r} (\alpha_{\text{aer}}(\lambda_R, r') + \alpha_{\text{mol}}(\lambda_R, r'))\, dr'\right]}{\exp\left[-\int_{r_0}^{r} (\alpha_{\text{aer}}(\lambda_0, r') + \alpha_{\text{mol}}(\lambda_0, r'))\, dr'\right]} \tag{15}$$

where P are the power received at the Raman wavelength, λ_R, and for laser wavelength, λ_0, at height r and calibration height r_0; N_R are the nitrogen molecules per volume unit; α_{aer} and α_{mol} the extinction

coefficients for Raman and laser wavelengths; and $\beta_{\text{mol}}(\lambda_0)$ are the molecular backscattering coefficients at height r and calibration height r_0.
The calibration height, r_0, was chosen such that the $\beta_{\text{aer}}(\lambda_0, r_0)$ term cancelled. This is because its value is not available from the data and it is possible to choose freely a height where the value is not needed. In the Barcelona Raman-LIDAR for 19th July 2018, the calibration point chosen was 5000 m, where from an extended Figure 6, it can be seen that the aerosol backscatter lines goes to zero.

In addition, there are statistical fluctuations of the Raman signal that can produce large fluctuations in the aerosol extinction profile and spread in the coefficient obtaining. These fluctuations can be prevented and corrected applying a mathematical regularization like the Savitzky-Golay filter applied in the case of this analysis.

3.3 Atmospheric aerosols

Aerosols have been described along this work as particles without a regular shape and with a messy structure. Moreover, aerosols in the atmosphere are composed of several elements, i.e., they are mixtures of many types of particles, they can be solid, commonly called water-insoluble, which have an amount of organic material, or liquid from a gas-to-particle conversion.

Aerosols form a heterogeneous layout around the Earth at given altitudes. Aerosols can have a natural or a human origin. It usually depends on the location of the Earth at which the atmosphere is being studied and on climatology conditions.
Aerosols are mainly classified as continental and maritime aerosols, but there are also other environmental events that produce aerosols. Places near the coast will be rich in sea-salt particles from ocean with solid and gas-liquid components. If the studied location is near to a city, aerosols basically are of urban haze or pollution, like soot from factories, cars and producers of carbon-rich elements. There are also environmental events like forest fire smoke which produce carbon sediments similarly to factories. Mineral particles, which form aerosols, are from arid regions, like deserts or tundras and snowy regions. These aerosols are transported over long distances and can be found in regions at thousands of kilometers of the natural source. In case of deserts, aerosol is basically dust composed by calcium, quartz and silicates from rocks and sand, but also iron, titanium and other kinds of heavy metals. Instead, in the case of tundras and snowy regions, the haze is composed mainly by sulfate and a solid-liquid component from frozen water.
Some regions can have a combination of several aerosol types from different locations. The atmosphere characterized through the Barcelona Raman-LIDAR, located in Barcelona, contains usually sea-salt aerosols, combined with urban haze, due to the short distance between the LIDAR station and the city. Depending on the season, desert dust from Sahara can be found, which is at about 2400 km from Barcelona. Particles are transported usually in spring and summer. Rarely, in winter, depending on cyclones, winds and other atmospheric conditions, snowy particles from northern regions can be detected.

Several studies, [14], [2], [15] have tried to classify the different types of aerosols by its physical characteristics. Through the tables that classify these aerosols and using the obtained coefficients by manipulated data, the atmosphere can be characterized in aerosol terms. There are different ways to analyze and classify aerosols, using a complex Mie scattering analysis or with the LIDAR ratio obtained from the extinction and backscattering coefficients.
Mie scattering is an analytic solution to Maxwell's equation for the scattering of electromagnetic radiation taking into account that the particles of aerosols are spherical among other approximations. This is a complex analysis with infinite sums of Bessel functions.
As said before, the LIDAR ratio is a relation between the extinction and backscattering coefficients which can be written as, α/β. The relation between them allows us to obtain several basic physical characteristics. When the LIDAR ratio has a smaller value means that the aerosols are small and opaques; and when the LIDAR ratio is bigger, the molecules are bigger and tend to be transparent.
The relation between the aerosol size and the LIDAR ratio can be explained visualizing the scattering of light on the particles. Two types of possible forms for aerosols are considered; a punctual form with a

smaller size than $\lambda/10$, and non-punctual particles with a size bigger than $\lambda/10$.

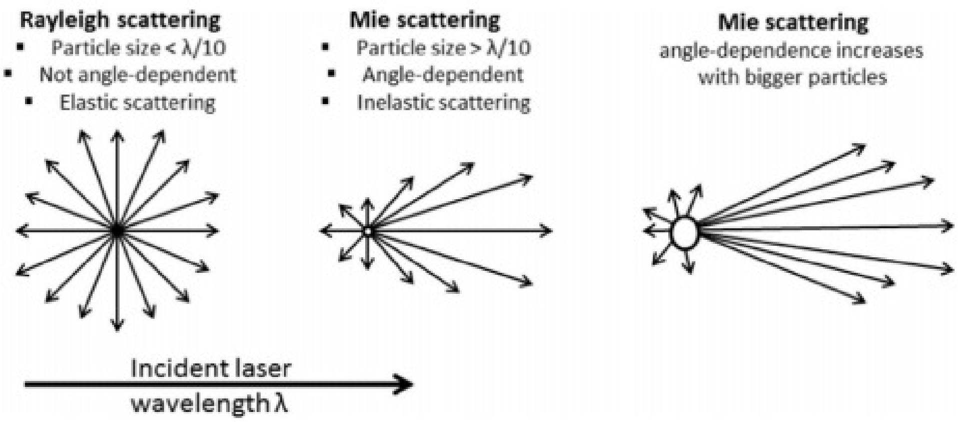

Figure 7: Schematic showing the differences between Rayleigh and Mie Scattering depending on the particle shape. [16]

Figure 7 shows the relation between the size of the aerosol and the type of scattering produced. Analyzing the punctual shape only Rayleigh scattering is produced and there is no dependence on the incidence angle except for a term $(1+\cos^2\theta)$. A bigger LIDAR ratio means a bigger particle because there exists a strong dependence with the angle. The bigger the particle, the more difficult it is to have a backscattering compared with the probability for scattering in any direction because of the angle term. Looking for the opacity level of the aerosol, it is easily deduced that when a particle is bigger and its backscattering coefficient is reduced, most of the light will be deflected in other directions or even cross the particle. If the biggest part of incident light goes through the particle, it will be more transparent than if the incident light which goes through the particle is smaller, being opaque in this case. Usually, a bigger particle whose LIDAR ratio is large, are more transparent than small particles. Therefore, using the LIDAR ratio previously obtained with the extinction and backscattering coefficient values, an analysis of the atmospheric aerosols can be done.

The study of atmospheric aerosols is important for many reasons. It is well known that greenhouse effect is one of the biggest problems of our time. Our carbon footprint is huge and humanity is causing irreversible damage. The aerosols found within the atmosphere have a negative contribution in greenhouse effect. These aerosols have an inhomogeneous distribution along the Earth, but its layer distribution in the atmosphere reduces the radiative heating of the Earth. Understand their impact on the global warming is therefore of great importance to know how its evolve along the time.

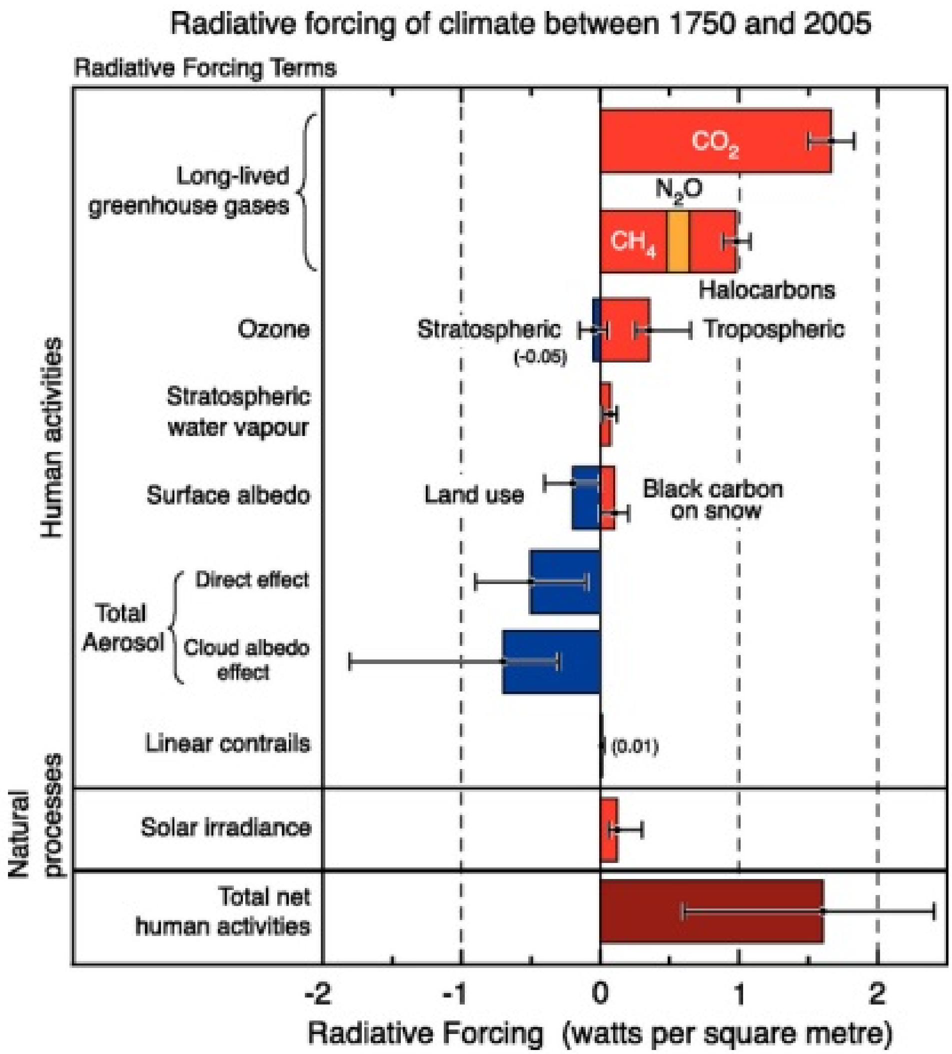

Figure 8: Analysis of radiative forcing of climate between 1750 and 2005 that shows the balance between the positive contribution, mainly by CO_2 and CH_4, and the negative contribution by some aerosols from clouds and other natural sources. [17]

Figure 8 shows, there is a negative contribution which reduce the radiative forcing that the Earth receives, reducing the greenhouse effect within a certain range with associated uncertainties. Accurate studies may help to know about these uncertainties and global warming using aerosol profiles. So, study the atmospheric aerosols profile is important to know to deal with the problem and improve the climate models.

3.4 Analysis of atmospheric aerosol composition through extinction and backscattering coefficients

By using a code in Pyhton programming language made by Scott Griffiths and Markus Gaug, which includes Eq. 14 and Eq. 15 expressions with the mentioned choice for the calibration height chosen at 5000 m, the extinction and backscattering coefficient were obtained. Furthermore, by using the obtained coefficients, the LIDAR ratio is obtained and the atmosphere can be described.

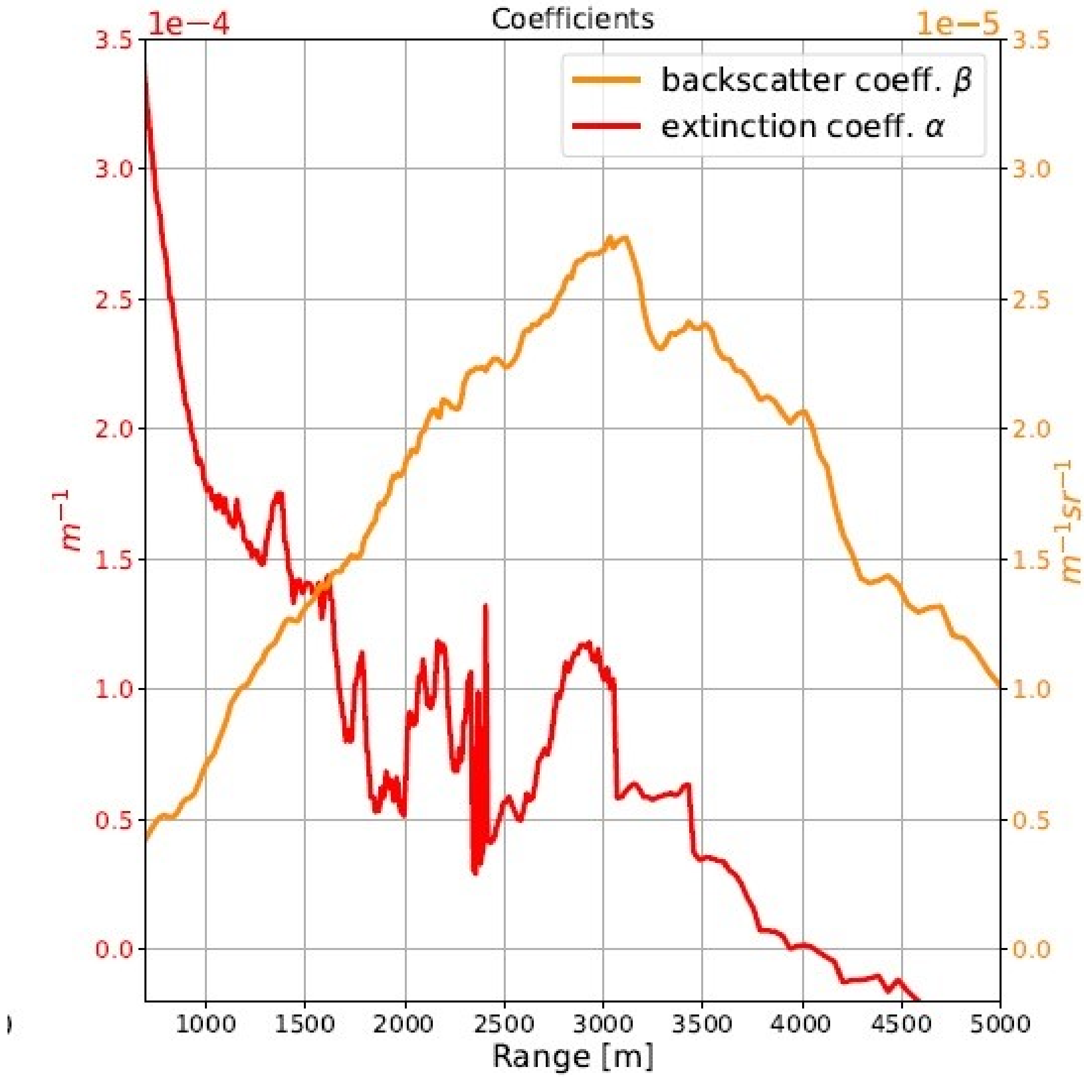

Figure 9: The extinction and backscattering coefficients evolution as a function of altitude of atmosphere at the UAB campus.

Figure 9 shows the evolution of extinction and backscattering coefficients as a function of altitude. The red line belongs to extinction coefficient, α, and the orange line belongs to backscattering coefficient, β. Looking for α, it decays from its maximum to a value a little below of zero due to statistical fluctuations and background noise from the system The physical meaning of this decay is because of the decrease of particles size with the growth of the altitude. In some points between 1500 and 3000 meters, the fluctuations manifest the presence of particles of multiple sizes depending on its origin.
Nevertheless, taking a closer look at β, the function shows an increase from the beginning up to 3000 meters, where a maximum is found. Its meaning is because of the decrease of particles size, there is

a greater possibility that the backscattering is produced due to the reduced angle dependence. After that maximum, the function decays because at high altitudes the density of particles decreases and less backscattering occurs.
As said before, the analysis shown in Figure 9 has implied systematic and statistics uncertainties, which are carried until the LIDAR ratio analysis. These carried uncertainties will be seen in 10 where LIDAR ratio fall to a null value.

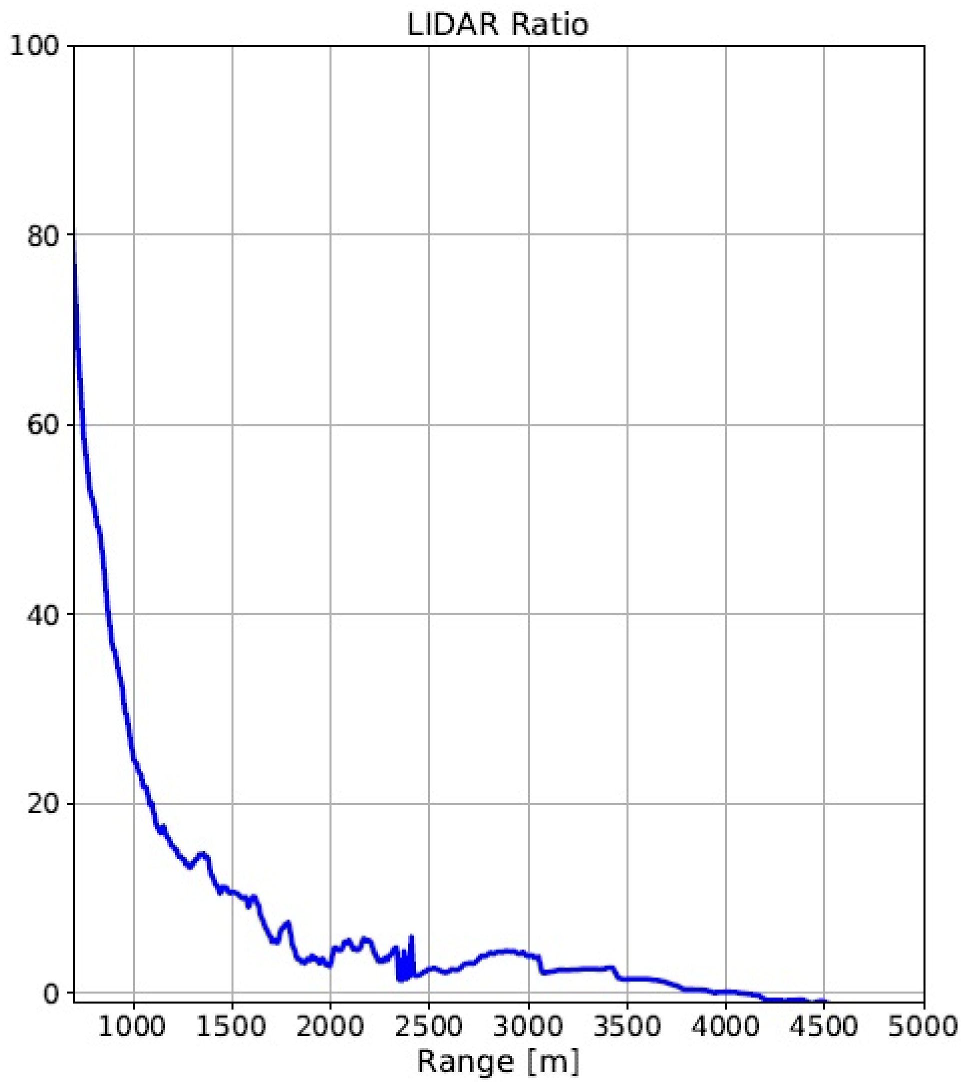

Figure 10: The LIDAR ratio evolution as a function of altitude of atmosphere above the UAB campus obtained through extinction and backscattering coefficients.

After taking a look at the coefficients evolution, the relation between the LIDAR ratio and the aerosolic profile can be analyzed and explained. As is known, the LIDAR ratio can be expressed as α/β. Using the results of extinction and backscattering coefficients shown in Figure 9, the LIDAR ratio profile is obtained and shown in Figure 10. Looking at its behaviour, an abrupt decay is produced at the first 2000 meters. This is because the extinction coefficient always decays with some fluctuation, while the backscattering coefficient increases up to a maximum at 3000 meters. This fast huge difference between the coefficients causes an abrupt decrease in LIDAR ratio values. From 2000 meters until the end, the decrease is smoother than before due to the β decrease, after its maximum, with α decreasing at a similar

rate.
It should be said that all the fluctuations that appear in Figure 10 come from α and β, i.e, are statistical fluctuations and system background noise. These carried uncertainties values make that the LIDAR ratio fall to a null value. This should not happen because of α and β, the LIDAR ratio can fall to a minimum of 8,33 Sr.
The LIDAR ratio only makes sense when the values of α and β are above 0. It is worth commenting that these values depend on which is the chosen r_0 leading to instabilities in this process. Moreover, in Figure 9 the coefficients have different absolute scales also affecting to Figure 10. So, LIDAR ratio have a minimum possible value of 8,3 Sr. Instead, some studies like [3], have obtained some LIDAR ratios with values below 0 due to coefficients uncertainties.
The code developed by Scott Griffiths and Markus Gaug is not finished yet, so the statistical and systematic uncertainties are not present in the analysis. Even so, these uncertainties can be approximated. The statistical uncertainty has a value at least ± 10, and the systematic uncertainty at least ± 10. Changing r_0 within reasonable ranges in Eq. 15 leads to change of ± 10 in LIDAR ratio.

Once shown the LIDAR ratio profile and its behaviour, the atmosphere can be characterized and its aerosols can be determined approximately. Some studies have established, after some experiments and analysis, a relation between the LIDAR ratio value and the type of aerosol found at a given height.
According to [2], Lidar and atmospheric aerosol particles, aerosols can be differentiated by their LIDAR ratio.

Table 1: Typical LIDAR ratios for different aerosol types at 532 nm wavelength determined with a Raman LIDAR extracted from chapter 4 of Albert Ansmann's thesis.

Type of aerosol	LIDAR ratio [Sr]
Marine particles	20-35
Saharan dust	50-80
Urban particles	35-70
Particles from biomass burning	70-100

Taking into account the values shown in table 1 and Figure 10 it is easy to see that in the first 1000 meters all kinds of aerosols can be found. Particles from biomass burning only survive in about the first 200 meters, these particles come from forest fires and carbon sources. However, urban particles easily reach altitudes of more than 1000 meters. As the study location is in Barcelona, marine particles can be found from the sea and be dragged several kilometers. The analyzed data taken in summer, so Saharan dust may be observed in the troposphere, too.
From 1000 meters until the end of the boundary layer at 2000 meters, only marine particles can be found with a lower density. Hereinafter, the aerosol type cannot be determined accurately. So, only the lower troposphere can be characterized at all.

4 Conclusions and outlook

The main goal of this work was the analysis and characterization of the atmosphere through the Barcelona Raman-LIDAR located at the Universitat Autònoma de Barcelona campus. During July 2018, the data was taken with the Raman-LIDAR after some stability studies of the LIDAR hardware.

The analysis was made by Markus Gaug, the director of this Bachelor thesis, with whom I collaborated since July 2018. From the collected data a day was chosen and processed through a code made by Scott Griffiths and Markus Gaug. The analysis revealed the backscattered signal received by the system with respect to the distance and other magnitudes like the wavelength, the temperature and the pressure. Using an ECMWF model a profile was obtained and filtered for Elastic and Raman lines. From this analysis we can see how the signal decays with height because of the aerosol and molecules density decrease. Moreover, Rayleigh scattering is produced due to the existence of an aerosol layer, represented by an increase of the signal in the first 3 km.

In order to characterize the atmosphere, the extinction and backscatter coefficients of the aerosols were obtained applying its expressions in the code. An important point on this process is to choose correctly the calibration point r_0 to cancel terms in the equation. The value of calibration point will have repercussion in the statistical uncertainties of the coefficients. After obtaining and plot the values of the coefficients in relation with the height, it is easily to see that the backscattering coefficient has a smaller value than extinction coefficient. However, the extinction coefficient decays to a minimum value while fluctuating and the backscattering coefficient increases its value up to a maximum at 3000 m. The increase of the coefficient values is related with the decrease of particles size, while the decrease of the value is related with the increase of particles size. According with the size of the particles, the probability of produce backscattering is bigger or smaller depending on the incidence angle. So we can think that from the beginning up to 3000 m the amount of particles with a small size is greater than the amount of particles with a big size. After 3000 m both of them decays because of the decrease of the density of particles with the height.

Once the coefficients were obtained, the LIDAR ratio profile can be obtained through them using the expression, α/β. The LIDAR ratio has an abrupt decay at the first 2000 m. Until the end, it has a smoother decrease. The obtained LIDAR ratio decays to 0 because of the uncertainties of the coefficients. Usually, the LIDAR ratio has a minimum value of 8,33 Sr but is possible to have a smaller value due to the carried uncertainties or instabilities when choosing r_0.
Using the table extracted from [2] and looking for the values at every height, we see that at the first 1000 m all aerosols can be found. Instead, when height is higher than 1000 m, only urban and marine particles can be found among other molecules. After the end of the boundary layer at 2000 m the aerosol type cannot be determined accurately. So, only the lower troposphere can be characterized at all.

In conclusion, the aerosols' layer can be characterized through the LIDAR ratio obtained with extinction and backscattering coefficients but only the lower troposphere can be characterized precisely.

References

[1] J. V. Jelley, "Cherenkov Radiation and its applications", Pergamon Press (1958) London.

[2] A. Ansmann and D. Müller, "Lidar and Atmospheric Aerosol Particles", Chapter 4 of "Lidar: Range-Resolved Optical Remote Sensing of the Atmosphere", C. Weitkamp Ed., Springer (2005) Berlin.

[3] A. Ansmann, M. Riebesell and C. Weitkamp, "Measurement of atmospheric extinction profiles with a Raman Lidar", Opt. Letters 15 (1990) p.746.

[4] E. Hecht,"Optics", Pearson Education Inc. (2017) United States of America.

[5] A. Bucholtz, "Rayleigh-scattering calculations for the terrestrial atmosphere", Applied Optics Vol. 34, No. 15 (May 1995) p.2765.

[6] S. Chandrasekhar, "Radiative Transfer", Oxford Univ. Press (1950) London.

[7] B. Bodhaine, N. Wood, E. Dutton and J. Slusser, "On Rayleigh Optical Depth Calculations", Journal of atmospheric and oceanic technology Vol. 16 (1999) p.1854.

[8] C. Tomasi, V. Vitale, B. Petkov, A. Lupi and A. Cacciari, "Improved algorithm for caluclations of Rayleigh-scattering optical depth in standard atmospheres", Applied Optics Vol. 44, No. 16 (June 2005) p.3320.

[9] S. Thornton and A. Rex, "Modern physics for scientists and engineers", Cengage Learning (2013) Boston, Massachussets.

[10] A. Ansmann, R. Neuber, P. Rairoux and U. Wandinger, "Advances in atmospheric remote sensing with Lidar", Selected papers of the 18th international Laser Radar conference (July 1996), Springer, Berlin.

[11] D. Müller, U. Wandinger, D. Althausen, I. Mattis and A. Ansmann, "Retrieval of physical particle properties from lidar observations of extinction and backscatter at multiple wavelenghts", Applied Optics Vol. 37, No. 12 (April 1998) p.2260.

[12] C. Fruck, "A new LIDAR system for the MAGIC telescopes and site search instrumentation for CTA", Max-Planck Institute, Diploma Thesis (February 2011).

[13] National Oceanic and Atmospheric Administration, National Aeronautics and Space Administration and United States Air Force, "U.S. STANDARD ATMOSPHERE", October 1976, Washington D.C.

[14] J. Ackermann, "The extinction-to-backscatter Ratio of tropospheric aerosol: a numerical study", American Meteorological Society (1998) p.1043.

[15] K. Kandler, N. Benker, U. Bundke, E. Cuevas, M. Ebert, P. Knippertz, S. Rodriguez, L. Schütz and S. Weinbruch, "Chemical composition and complex refractive index of Saharan mineral dust at Izaña, Tenerife (Spain) derived by electron microscopy", Atmospheric Environment (2007) p.8058-8074.

[16] S. Bhattacharjee, "DLS and zeta potential- What they are and what they are not?", School of veterinary medicine (2016), University College Dublin, Dublin, p.337-351.

[17] F. Guzmán, "Atmospheric vertical profiling by raman lidar", Ph.D. Dissertation, Universidad de Granada (June 2011).